water

MDPI

Article

Influence of Radical Scavenger on Radiation Synthesis of Graphene Oxide/TiO_2 Nanotubes/Ag Nanoparticles Nanocomposites and Their Dye Photodegradation Efficiency

Anh Phuong Thi Nguyen [1], Thuy Thanh Thi Nguyen [1,2] and Khoa Dang Nguyen Vo [1,2,*]

[1] Institute of Applied Materials Science (IAMS), Vietnam Academy of Science and Technology (VAST), Ho Chi Minh City 700000, Vietnam; ntpanh@iams.vats.vn (A.P.T.N.)
[2] Graduate University of Science and Technology (GUST), Vietnam Academy of Science and Technology (VAST), Hanoi 100000, Vietnam
* Correspondence: vndkhoa@iams.vast.vn; Tel.: +84-909622589

Abstract: Aqueous solutions of graphene oxide (GO), TiO_2 nanotubes (TNTs), and silver nanoparticles (AgNPs) were synthesized through a facile, single-step radiolytic method at room temperature and ambient pressure. The resulting material, referred to as GO-TNTs-AgNPs (GTA), was investigated for its potential application in the photodegradation of Rhodamine-B (RhB) dye. This synthesis process relies on the interaction of high-energy gamma rays from a ^{60}Co source with the water in the aqueous solutions. The main objective of this study was to evaluate the effect of irradiation dose and the presence of polyethylene glycol (PEG) solution on the combination within the nanocomposite materials. The inefficiency of GTA synthesis experimentally was in agreement with the hydroxyl radical (HO•) scavenger. Then, the irradiated materials were structurally characterized using various spectroscopic methods (Fourier transform infrared (FTIR), X-ray diffraction (XRD), Raman spectroscopy, and ultraviolet-visible absorption (UV–Vis)). Scanning electron microscopy (SEM) studies reveal the variable morphology of nanocomposites. GTA samples in water exhibited significantly higher degradation efficiency on Rhodamine B dye under natural sunlight irradiation conditions.

Keywords: graphene oxide; TiO_2 nanotubes; radiation; photodegradation; dye treatment

Citation: Nguyen, A.P.T.; Nguyen, T.T.T.; Vo, K.D.N. Influence of Radical Scavenger on Radiation Synthesis of Graphene Oxide/TiO_2 Nanotubes/Ag Nanoparticles Nanocomposites and Their Dye Photodegradation Efficiency. *Water* **2023**, *15*, 2799. https://doi.org/10.3390/w15152799

Academic Editor: Alexandre T. Paulino

Received: 10 July 2023
Revised: 26 July 2023
Accepted: 30 July 2023
Published: 2 August 2023

1. Introduction

Water contamination primarily resulting from organic dyes (emanating from the dyeing, printing, food, textile, and leather industries) is garnering increasing concern. Numerous dye variants are recognized as carcinogens and cannot undergo decomposition [1,2]. As a result, the development of advanced nanocomposite materials for effective dye removal is an actively examined subject. Recently, treatment technologies have been developed to address water and sewage pollutants, and photocatalysts have been extensively investigated due to their purity, recyclability, environmental friendliness, and high efficiency.

Composite materials with environment treatment properties synthesized from advanced materials on the basis of carbon have recently garnered significant attention. Graphene oxide (GO) exhibits numerous oxygenated groups, including hydroxyl (–OH), epoxy (–O–), carbonyl (–C=O), and carboxyl (–COOH) groups, dispersed throughout the basal planes [3]. These functional groups enhance GO's reaction ability, interlayer distance, conductivity, thermal conductivity, and hydrophilic effect compared to graphite and graphene. As reported by Xiaoman Lei et al., GO is commonly used as a substrate for binding nanoparticles [4]. GO and TiO_2 nanotube nanocomposites were synthesized using a one-step hydrothermal method, resulting in a 97% degradation of methylene blue dye under UV irradiation. GO enhances light absorption and photocatalytic activity by

mitigating charge recombination when functioning as an electronic transmission catalyst [5]. Furthermore, according to Kumari et al., a combination of silver nanoparticles and GO was successfully achieved using an ultrasonic method combined with heating at 400 °C and rapid cooling to −20 °C. The results demonstrate that this nanocomposite exhibits reversible properties. Notably, GO has emerged in recent years as an advanced substance for wastewater treatment due to its cost-effectiveness in production, expansive surface area, and effective interaction with various anionic, cationic, or neutral dyes in aqueous environments [6].

Recently, the photocatalytic degradation surpassed the conventional methods in water treatment; therefore, the TiO_2-GO composite attracted enormous interest from several researchers. TiO_2 nanotubes, derived from TiO_2 nanoparticles in the anatase phase, possess compact structures and exhibit a specific surface area five times greater than that of their precursors [7]. They demonstrate excellent photocatalytic effects and are well-suited for materials requiring efficient dye processing. The electrochemical process occurs directly on the titanium surface, creating numerous active sites that enhance electron transmission intensity [8]. However, the band gap of TNTs is 3.17 eV, which has led to the incorporation of nanoparticles in many studies to enhance the photocatalytic activity for dye decomposition [9,10]. These nanoparticles enable the absorption of low-energy photons, thereby generating additional electron–hole pairs within the TNT bandgap [11].

Among the TNTs combined nanoparticles, silver nanoparticles are renowned for their exceptional and multifaceted physical, chemical, and biochemical characteristics, including antibacterial properties, optical attributes, high electrical conductivity, and catalytic activity. The incorporation and arrangement of AgNPs alongside carbon-based materials (such as carbon nanotubes, graphene oxide, and graphene) as well as TNTs establish a robust connection between these two materials, rendering them highly applicable in the field of photochemistry [12,13].

Diverse available processes for the synthesis of the TiO_2-GO nanocomposite, Ag/TiO_2 nanocomposite Ag-rGO-TiO_2 have already been investigated, though mainly through thermal and chemical methods [14–16]. γ-ray interaction, an efficient energic source, can lead to the ionization and excitation of molecules and atoms within the substrate through various possible pathways, resulting in the formation of e^-_{aq}, HO•, H•, H_2O_2, H_2, H^+, OH^-, and other reactive species. Hydrated electrons (e^-_{aq}) and hydrogen atoms act as potent reducing agents while the hydroxyl radical (HO•) functions as an oxidizing agent [17]. The benefits of utilizing radiation involve the potential to manipulate substrates in any physical state at ambient temperature, typically without the requirement of any additional catalysts or other substances. The interaction of this high-energy radiation with organic monomers and polymers triggers diverse chemical changes of increasing significance from both scientific and technological perspectives. Cross-linking and scission in polymer networks, attaching onto synthetic and natural polymers as well as the chemical stimulation of organic substances through oxidation, can be induced by irradiation under soft conditions [18]. For the metal nanoparticles synthesized, among the entities produced by water radiolysis, e^-_{aq} and hydrogen atoms possess potent reducing capabilities that can convert metal ions into clusters of metal with zero valence [19]. Jingye Li et al. [20] hypothesized that the generation of reductive radicals through γ-radiolysis of solvents is the primary mechanism responsible for the reduction of oxygen and restructuring of GO sheets, resulting in reduced GO (rGO). The main difference between GO and rGO is considered to be the electrical conductivity, which opens up different possible applications for the two materials.

Based on available information, several published investigations have been conducted on the radiation synthesis of nanocomposite materials using reactive species and stabilizers. However, the role of radio hydrolysis reactive species particularly in the combination of GO, TNTs, and AgNPs has not been completely appreciated. Further research is needed to explore the multidimensional and simultaneous effects that occur during the irradiation of the precursors. In this study, the GO-TNTs-AgNPs composites (labeled GTA) were prepared

by employing γ-ray on a ^{60}Co source in aqueous media whilst a radical scavenger was utilized to establish a reducing environment for chemical reactions. The role of polyethylene glycol (PEG) in scavenging HO• aims to elucidate the influence of γ-ray irradiation on the synthesis of GTA in two different solvents: pure water and a PEG solution. Then, the RhB photodegradation performance of these GTA materials was investigated in support of the synthesis results. Rhodamine B was chosen because it is used as one of the common targets for nanocomposite's photodegradation properties [21–23].

2. Materials and Methods

2.1. Reagents

Graphite powder (99.9%) was purchased from Acros Organics (Germany); TiO_2 anatase nanopowder (99.9%), nitric acid (65%), and $AgNO_3$ (>99%) were purchased from Merck (Darmstadt, Germany). RhB dye (98.0%) was purchased from HiMedia, Mumbai, India. Other analytical-grade chemicals were used without further purification.

2.2. Radiation of GO-TNTs-AgNPs

Before the irradiation, TNTs were synthesized by the method of Zavala Ávila et al. using TiO_2 anatase nanopowder as a precursor [24]. The product TNTs was vacuum dried to obtain the powder form. AgNPs were prepared from silver nitrate with an anti-agglomeration polymer instead of poly (sodium styrene sulfonate), which is polyethylene glycol [25]. This solution was sealed and kept in the dark for further procedures. Graphene oxide (GO), with graphite powder as the precursor and $KMnO_4$ as the oxidizing agent, was synthesized using improved Hummer's method [26]. The product, GO, was vacuum dried for further synthesis.

Before the synthesis of GO-TNTs-AgNPs material, the separated two-component composites, namely GO-TNTs and AgNPs-TNTs, were investigated, and the suitable ratio for the three-component combination was 2:1:2 (*w*/*w*/*w*). First, GO solution (2%), TNTs solution (1%), and AgNPs solution (2%) were prepared in water and in a 0.5 g/L PEG solution. Then, appropriate amounts of the three solutions in two different media were mixed separately in a 100 mL flask and sonified for 15 min. The GO-TNTs-AgNPs 2:1:2 samples were subjected to γ-ray irradiation at VINAGAMMA Center (Ho Chi Minh City, Vietnam) on a ^{60}Co source with a dose rate of 1.1 kGy/h measured by the ethanol-chlorobenzene dosimetry system (ISO/ASTM 51538-2009). Doses varied between 5 kGy and 15 kGy. After irradiation, the samples were stored at room temperature for 24 h before analysis. The final samples were labeled as GTA-0-W, GTA-5-W, GTA-15-W (in Water), GTA-0-P, GTA-5-P, and GTA-15-P (in PEG).

After undergoing irradiation with varying doses of γ-ray, all nanocomposites solutions were acquired in the form of dark brown solutions (Figure 1).

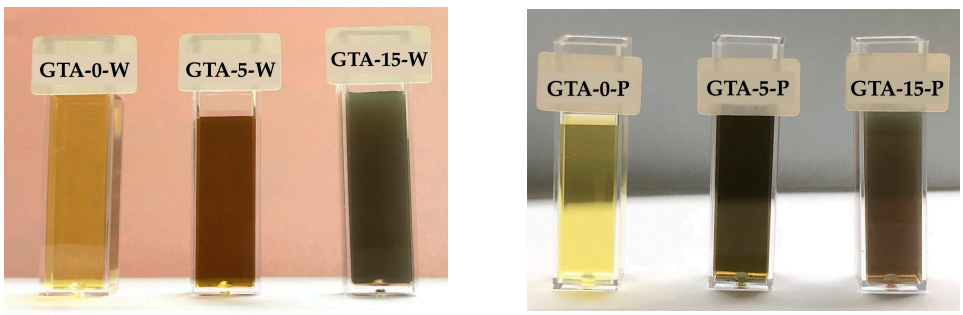

Figure 1. Fabricated nanocomposite GTA-0-W, GTA-5-W, GTA-15-W (in Water), GTA-0-P, GTA-5-P, and GTA-15-P (in PEG solution); before irradiation, at 5 kGy and 15 kGy.

2.3. Materials Characterization

The crystalline structure, morphology, and properties of the resulting GTAs were characterized using X-ray diffraction, Fourier transform infrared spectroscopy, Raman spec-

troscopy, ultraviolet-visible adsorption, and Scanning electron microscope (FE-SEM-S4800—Hitachi, Tokyo, Japan). FTIR spectra were collected using a MIR/NIR Frontier spectrometer (PerkinElmer, Waltham, MA, USA) within the wavenumber range of 4000–400 cm^{-1}, KBr pellets were prepared with 5 mg of each GTA nanocomposite sample, and the average scanning speed was set to 30 scans/min. UV–Vis absorption spectra were recorded using a UV-1800 spectrometer (Shimadzu, Kyoto City, Japan) with a scanning speed of 50 nm/min and a wavelength interval of 0.1 nm. Raman spectra were obtained with an XploraOne spectrometer (Horiba, Kyoto City, Japan) using a laser wavelength of 532 nm and a grating of 900 gr/mm. X-ray diffractograms were acquired using a D2 Phaser diffractometer (Bruker, Germany) with a scanning speed of 0.026355 degree/s and Cu/Kα as the X-ray source.

Prior to assessing the photocatalytic capability of the sample, it was essential to determine the precise content of each component (GO-TNTs-AgNPs) using the Inductively Coupled Plasma-Mass Spectrometry (ICP-MS) method on NexION®2000–PerkinElmer America. All samples were weighed to 5 mg and dissolved in a heated solution of 65% HNO_3 and 10% HF, which aided in the better dissolution of TNTs.

2.4. Rhodamine B Dye Photodecomposition

First, the concentration of RhB in untreated solution ($[RhB_{initial}]$) was recorded as shown in Figure 2. The spectrum indicated that the peak absorption of the 10 ppm RhB solution occurred at a wavelength of 553.5 nm. This wavelength was then utilized to construct a standard curve for RhB, encompassing five concentrations of 2, 4, 6, 8, and 10 ppm. The resulting equation for RhB was determined as y = 0.2092x + 0.0086, with R^2 = 0.99966.

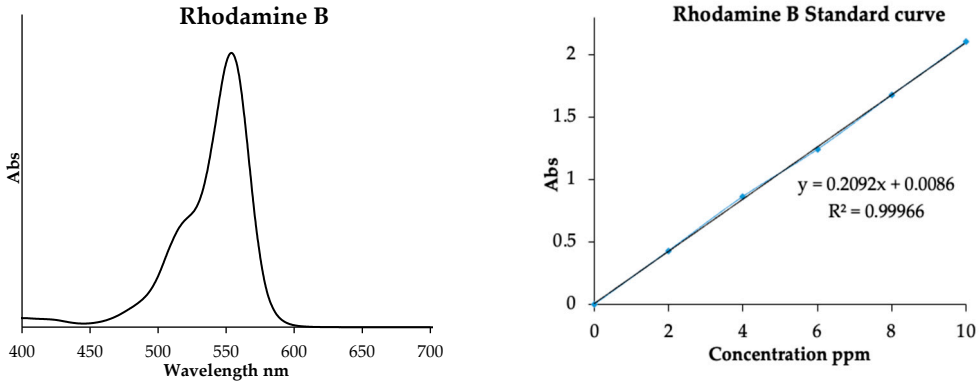

Figure 2. UV–Vis absorption spectrum of Rhodamine B and its calibration curve.

The photodecomposition of RhB dye was conducted as follows: 4 mg of each GAT nanocomposite sample was mixed with 10 mL of a solution containing 10 ppm RhB. The experiment was performed between 11:00 a.m. and 1:00 p.m., utilizing the highest natural UV–Vis energy available.

For initial materials (TNTs and AgNPs), the highest density value of each component attained from ICP-MS analysis will be utilized to determine the individual amount for the photocatalytic reaction. The amounts were calculated as follows [27]:

$$\text{Weight (mg)} = (p \times 4)/100 \quad (1)$$

where p (in %) represented the highest content of each precursor in the nanocomposite obtained from ICP-MS analysis, and 4 denoted the weight of nanocomposite samples (in mg) used in the photodegradation experiment.

After the photocatalysis process, the sample was passed through filter paper, and the concentration of RhB was subsequently determined using the RhB calibration curve.

The photocatalytic activity was assessed based on the decolorization efficiency (DE, %), calculated using the following formula [28]:

$$DE(\%) = \left[1 - \frac{C}{C_0}\right] \times 100 \quad (2)$$

where C_0 (ppm) was the initial dye concentration, and C was the dye residue concentration after photocatalytic reaction.

3. Results

3.1. Effect of the Irradiation Dose and a Radical Scavenger on GTA Synthesis

The ultraviolet–visible (UV–Vis) spectra of GO exhibit two absorption peaks at 250 nm and 289 nm [29] while the absorption band of TNTs ranges from 250 nm to 300 nm [24], and AgNPs display an absorption peak at 385 nm [25]. In the two samples, GTA-0-W and GTA-0-P, the spectra display three distinct absorption peaks corresponding to the initial materials, with the absorption peak of AgNPs observed at 400 nm. The sample GTA-5-W exhibits three absorption bands with a slight red shift, indicating an increase in the size of AgNPs [30]. Moreover, the broadening of the absorption bands of GO sheets and TNTs compared to their pre-radiation states suggests the formation of Ti-O-C bonds [31]. Additionally, increasing the irradiation dose up to 15 kGy may lead to AgNPs agglomeration, resulting in a reduced absorption intensity and a color change of the solution from yellow–brown to dark brown, which aligns with the findings of Wang et al. [32]. Similar trends can be observed in the GTA-PEG sample, where the intensity of the absorption peak sharply decreases and its shape broadens (Figure 3).

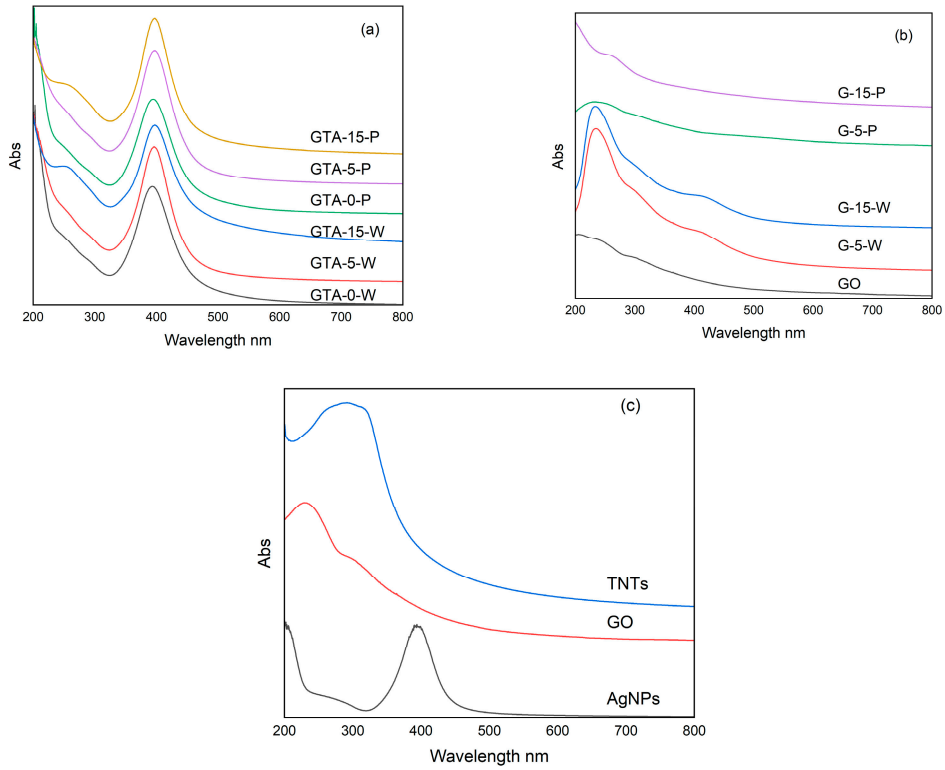

Figure 3. UV–Vis spectra of (**a**) GTA samples and (**b**) GO at dose 0 kGy, 5 kGy, 15 kGy, (**c**) precursors.

Figure 4 shows the FTIR spectra of irradiated GO, GTA composites and their precursors. The peak observed at 3400–3600 cm^{-1} corresponds to the hydroxyl group (–OH) present in both PEG and GO. The peak at 2900–3150 cm^{-1} indicates the vibration of the O–H bond in carboxylic acid (Table 1). The peak at 1632 cm^{-1} signifies the vibration of the C=C bond and Ti-OH bond [33] while the vibrations of the C=O bond and C–C bond

from the aromatic ring are observed at 1711 cm^{-1} and 1435 cm^{-1}, respectively [34]. Upon exposure to gamma rays, the absorption peaks changed, indicating the interactions within the materials. Among the three compositions in GTA, the GO scaffold was the most affected element, which was susceptibly reduced under the irradiation condition since TNTs and AgNPs existed as nanoparticles before irradiation. The intensity as well as the position of characteristic function groups vibration in GO moderately varied; in particular, the transmittance of the peaks increased at 3400–3600 cm^{-1} (–OH), 1730 cm^{-1} (–C=O), and 1621 cm^{-1} (C=C) and decreased at 1085 cm^{-1} (C–O) (Figure 4b). The radio-reduction effect on GO gradually rises with the dose; consequently, GO irradiated under 15 kGy performed the hydrophilicity (Figure 1). Moreover, the literature and experimental results also demonstrate that various radiation media influence the reduction of GO differently; in this study specifically, the chemical structure of GO was significantly altered by the γ-ray in water compared to a low-concentration PEG solution.

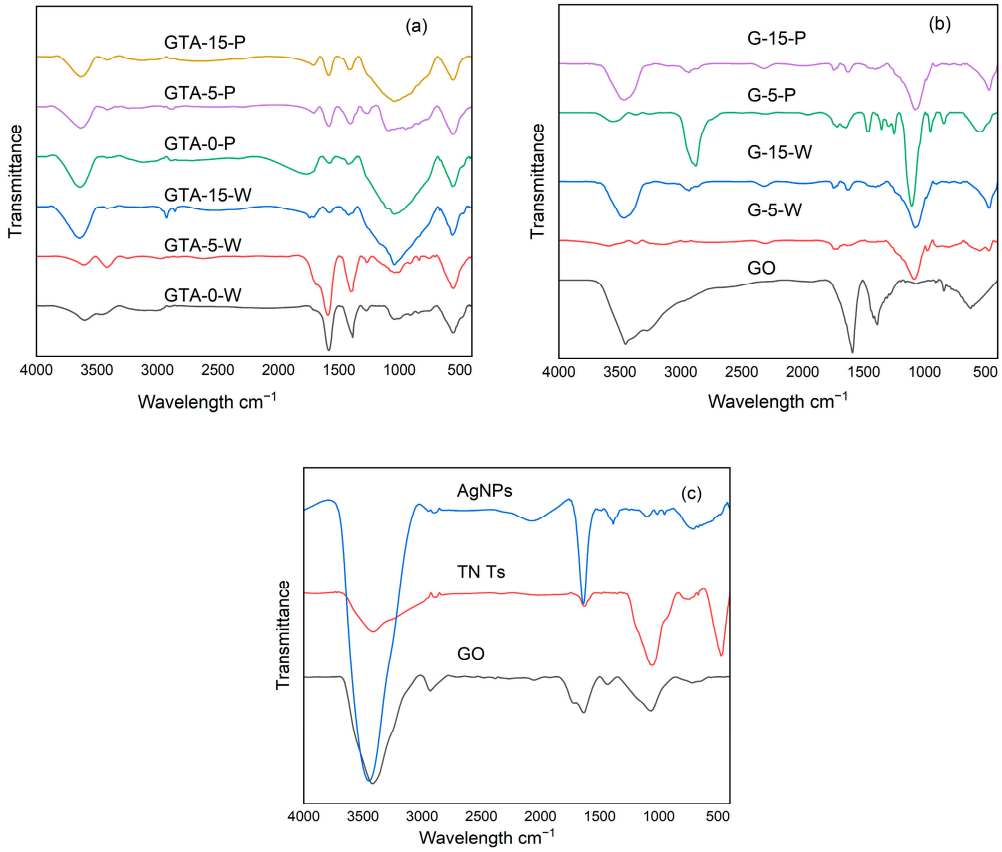

Figure 4. FT-IR spectra of (**a**) GTA samples and (**b**) GO at dose 0 kGy, 5 kGy, 15 kGy and (**c**) precursors.

Table 1. FTIR data of GTA composite.

Experimental FTIR (cm^{-1})	Literature	Vibration Mode
3640–3310	3640–3200	H bonded O–H stretch
3309–2805	3300–2500	C–H stretch in aromatic O–H stretch carboxylic acid
1698	1760–1690	C=O stretch
1591	1600–1585	Ti–OH, C=C
1480	1500–1400	C–C stretch in ring
1272, 1035	1320–1000	C–O stretch in carboxylic acid
916	950–916	O–H bend in carboxylic acid
553	600–400	Ti–O–Ti

In the GTA sample prepared with water as the solvent, the peak intensities at 1600 cm^{-1} and 1420 cm^{-1} are significantly reduced at a dose of 15 kGy, and the absorption region at 750–1400 cm^{-1} enlarges due to the GO-TNTs and Ag–O interactions during irradiation. Additionally, a decrease in peak intensity at 1500–1700 cm^{-1}, corresponding to the C=O bond, indicates the bonding of AgNPs and TNTs onto the GO surface [6].

In the GTA sample prepared in the presence of PEG, the magnitude of the vibration of the O–H group at 3400–3600 cm^{-1} is reduced because of the PEG radiation impact on GO. This could be attributed to the removal of some free radicals generated by water during PEG irradiation while the remaining free radicals interact with the surface of GO, leading to a reduction in the hydroxyl functional group [35]. Moreover, the absorption peak at 1750 cm^{-1} increases due to the C=O group formed by the oxidation of PEG by those water radiolysis free radials. The photodegradation efficiency of the investigated TiO_2 samples is additionally validated through the alterations in the absorption peak of hydroxyl vibration [36]. The FTIR spectra of GTA under irradiation provide a suitable basis for elucidating the observed phenomena.

The Raman spectrum (Figure 5) aligned closely with the conclusions drawn from FTIR and UV–Vis spectra. This spectroscopic method is an integral technique mostly used to feature graphene based materials, particularly two fundamental vibrations, namely the D band and G band, observed (at ~1350 and ~1600 cm^{-1}). The D-band vibration corresponds to disordered or defective regions caused by the presence of hydroxyl and epoxy functional groups. On the other hand, the G band vibration arises from sp^2 carbon atoms, representing E_{2g} phonons [37]. The Raman experimental results of GO once again confirm the strong radio-reduction effect on GO in water medium than in PEG solution via the increase of the I_D/I_G ratio in irradiated samples.

The I_D/I_G ratio of the GTA-5-W sample (Figure 5a) decreases compared to that of the mixture before irradiation. This reduction may be attributed to the absence of physical bonds between AgNPs, TNTs, and GO. However, at an irradiation dose of 15 kGy, AgNPs become stabilized and can adhere to TNTs and GO. This leads to an enhancement of the D band vibration, a sharp increase in the I_D/I_G ratio, and potentially the formation of Ti–O–C bonds [38]. When the synthesis was conducted in a PEG solution, the reduction of free radicals by the PEG scavenger had a great impact on the crosslinking between the initial materials, resulting in a decrease in the I_D/I_G ratio. Therefore, the Raman spectrum provides insights into the interactions among the three materials, which are more pronounced when water is used as the solvent, as evidenced by the shifting of the D band and G band.

In regard to the TNT component, its sole Raman spectrum (Figure 5c) indicates all characteristic peaks at 144 cm^{-1} ($E_{g(1)}$), 197 cm^{-1} ($E_{g(2)}$), and 642 cm^{-1} ($E_{g(3)}$); 397 cm^{-1} ($B_{1g(1)}$); and 520 cm^{-1} A_{1g}, $B_{1g(2)}$ cm^{-1} [39]. However, these peaks dramatically declined when TNTs were associated with AgNPs and GO in their mixtures as well as in nanocomposites, suggesting the encapsulation of GO over the other two ingredients.

XRD patterns continued to support the above-mentioned spectroscopic results. The diffractograms of mixed samples show characteristic peaks and crystalline nature of three components, reflections attribute to GO at $2\theta = 10.8°$, (001) plane; TNTs at $2\theta = 25.8°$, 38.4°, and 48.5° corresponding to (101), (004), and (200) planes, respectively (Anatase: JCPDS No. 65-5714), at $2\theta = 27.3°$, (100) plane (Rutile: JCPDS No. 21-1276), at $2\theta = 28.5°$, 46.5° as (121) and (200) planes (Brookite: JCPDS No. 29-1360); and AgNPs (at $2\theta = 33.5°$, 38°, 65° corresponding to (101), (111), (200) planes, respectively (JCPDS No. 65-2871)) [39,40]. For the samples prepared in water, after irradiation, the intensity of these peaks decreases. Specifically, at 15 kGy dose, two peaks at $2\theta = 38.4°$ related to TNTs and AgNPs at $2\theta = 48.5°$ attributed to TNTs intensively increasing while the other diffraction peaks of the initial materials diminished, and their baselines are also lowered (Figure 6a). These findings indicated that the GTA composites were successfully synthesized under water irradiation at 15 kGy and the combination of the precursors affected the crystal structures of the initial materials, accounting for the obscurity of their diffraction planes [41].

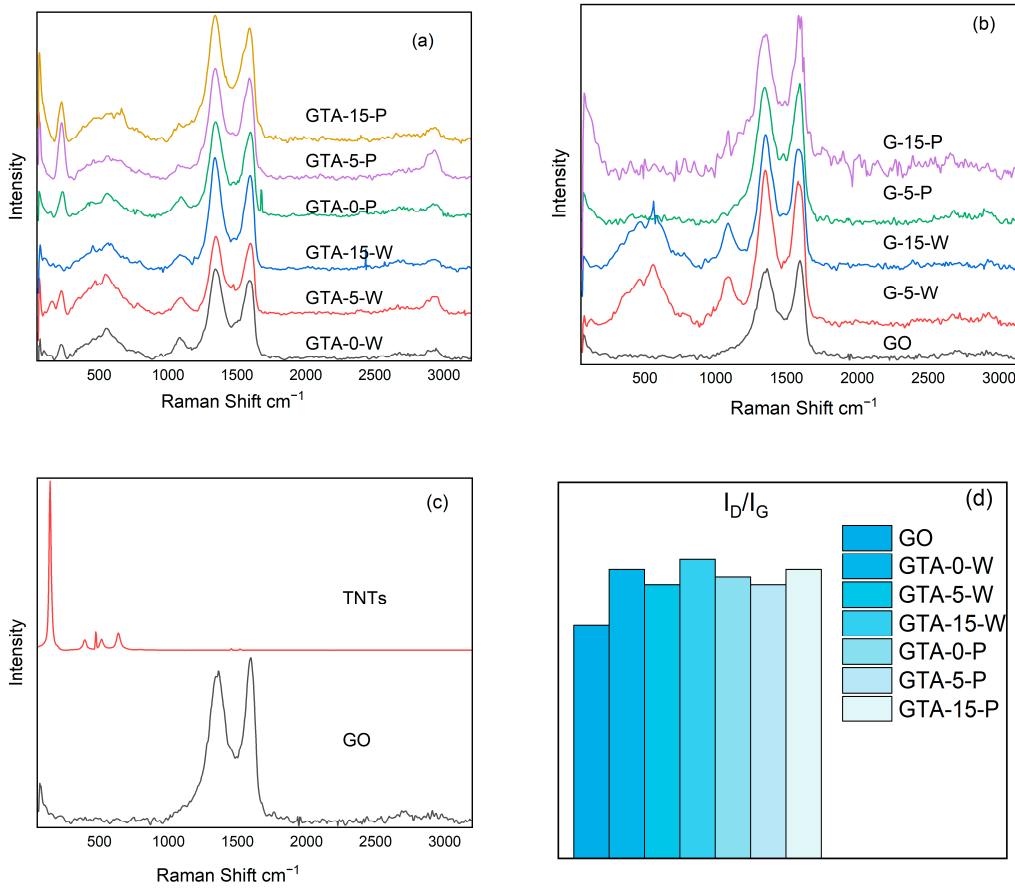

Figure 5. Raman spectra of (**a**) GTA samples, (**b**) GO at dose 0 kGy, 5 kGy, 15 kGy (**c**) precursors and (**d**) I_D/I_G ratio.

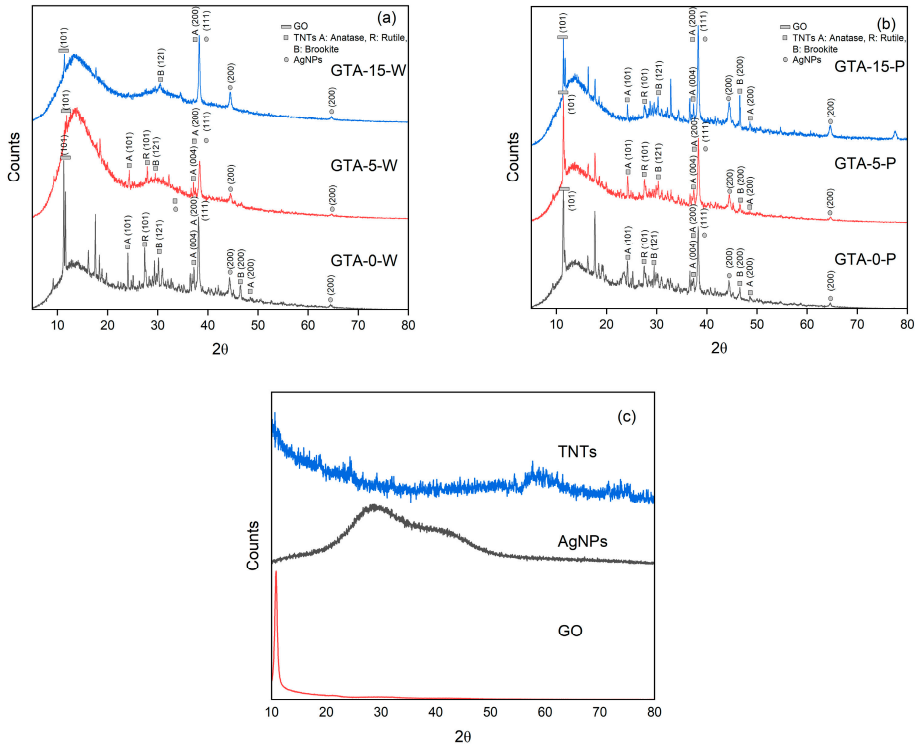

Figure 6. XRD patterns of GTA samples (**a**) in water and (**b**) in PEG and (**c**) precursor.

Apparently, X-ray diffractograms illustrate the more efficient radio synthesis of GAT in pure water than in PEG medium. When PEG was used as the solvent, small changes are observed, and the characteristic peaks of the starting materials could be individually identified (Figure 6b). Nonetheless, the 15 kGy dose also manifests the productivity of incorporating the three components.

In order to further elucidate the spectroscopic results, SEM images in Figure 7 exhibit the interaction between GO, AgNPs, and TNTs. In the samples before irradiation and at a 5 kGy dose (Figure 7a,b,d,e), only the GO can be clearly observed, though its surficial morphology in the irradiated samples was modified and became smoother as a result of the radio reduction. Remarkably, in GTA samples at 15 kGy (Figure 7c,f), the images reveal small white aggregations and several minuscule dots, presumably indicating the arrangement of TNTs clusters and AgNPs, enveloping the external surface of GO layers. However, the geomorphologic structure of GTA prepared in water appeared more sharp in comparison to GTA prepared in PEG, as a consequence of the sticking of PEG on the composites surface.

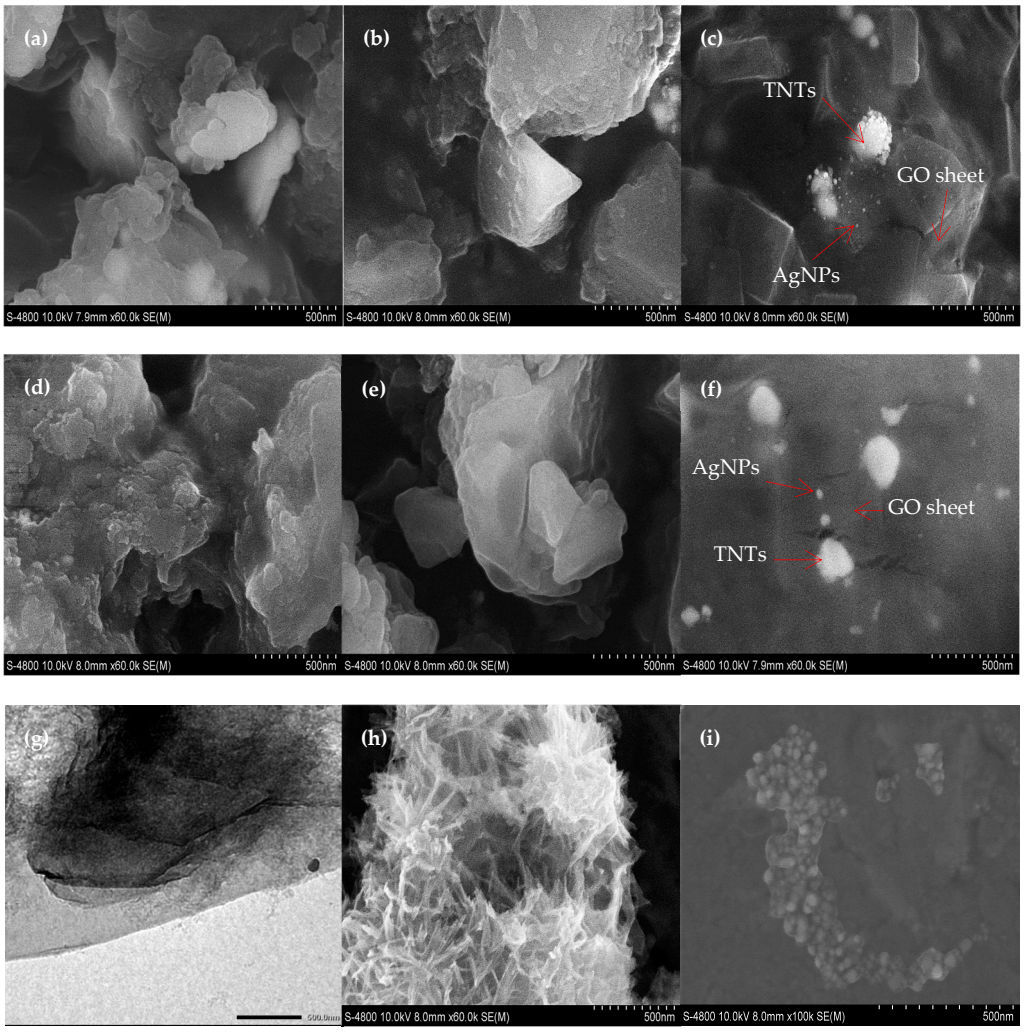

Figure 7. SEM images of (**a**) GTA-0-W, (**b**) GTA-5-W, (**c**) GTA-15-W, (**d**) GTA-0-P, (**e**) GTA-5-P, (**f**) GTA-15-P, (**g**) GO, (**h**) TNTs, and (**i**) AgNPs.

The obtained findings regarding the assistance of gamma irradiation in the GTA nanocomposite synthesis denote that the irradiation dose and the presence of a radical scavenger have certain effects on the chemical interactions among GO, TNTs, and AgNPs. The scavenging of HO• radicals results in a decrease in the presence of the oxidizing agent.

These results suggest that the release of HO• radicals during irradiation plays a crucial role in the attachment between GO, TNTs, and AgNPs. In the case of PEG, which acts as a radical scavenger, the cohesion among GO, TNTs, and AgNPs is not as strong as in the water case. As the irradiation dose increases, the signals become stronger, although the change is not as significant as in the PEG case. This result can be explained by the impact on the RhB photodegradation capacity of GTA prepared in water and in PEG solution.

3.2. Effect of the Irradiation Dose and a Radical Scavenger on Photodecomposition Ability of GAT

The capacity of RhB photodegradation in GTA composites supposedly relies on the TNTs and AgNPs compositions. The proportion of TNTs and AgNPs in GTA nanocomposites was calculated based on their concentrations obtained from the ICP-MS results (Table 2).

Table 2. Proportion of AgNPs and TNTs in GTA nanocomposites.

Samples Name	AgNPs (%)	TNTs (%)
GTA-0-W	7.73	21.25
GTA-5-W	8.49	14.75
GTA-15-W	7.50	8.00
GTA-0-P	5.28	3.75
GTA-5-P	11.74	9.50
GTA-15-P	7.08	22.95

In order to investigate the impact of γ-rays in two media on the structural changes of GTA, their behavior of photodegradation for RhB was evaluated. The aforementioned observations can be attributed to the fact that an augmentation in TiO_2 and hydroxyl radicals, and the structure area of crystallites can function as an impurity, diminishing recombination and augmenting the photodecomposition efficacy.

The results in Figure 8 point out that the pre-irradiated mixtures exhibited higher dye removal activity than the GAT at 5 kGy, and the samples at 15 kGy possessed the highest effectiveness, notably all exceeding that of the starting material TiO_2. The attained result can be explained by the fact that before irradiation, the high potential adsorption of the GO sheets promoted the RhB removal ability, after irradiating at 5kGy, surficial function groups on GO were modified, resulting in a slight DE decrease. The great improvement in the photodegradation performance of the GTA nanocomposite with a 15 kGy irradiation dose can be attributed to the increased crystallization of the TiO_2 and the affiliation of AgNPs components, which leads to three components synergistic outcomes [42]. This explicates that the attachment between the three precursors rather than their proportion plays the pivotal role in the photodegradation ability of the GTA composites; as demonstrated by the obtained experimental data shown in Table 2, the real amount of TiO_2 in GTA fabricated in PEG (GTA-15-P) was much higher than that in GTA fabricated in water (GTA-15-W). The administered dose in this study was kept low, with the intention of effectively amalgamating the precursors, as the GO was reduced by gamma-ray irradiation to the rGO for 35.3 kGy [20]. Additionally, the radiation media also influences the interaction among GO, TNTs, and AgNPs, which clarifies the highest photodecomposition activity exhibited by GTA-15-W. In water medium, the oxidative HO• can influence both TNTs and AgNPs; in addition, the chemical modifications occurring on the surface of TNTs due to ion, electron, and neutral species of gamma-irradiation led to an augmentation of Ti and hydroxyl radical, thereby promoting the progress of photocatalytic performance [43]. This interpretation is supported by the photodegradation effectiveness of samples in water. In the presence of a radical scavenger during irradiation, the removal of the oxidative agent (HO•) by PEG creates a more favorable reducing environment provoked an ineffective attachment between the three materials, resulting in a fall-off in the photocatalytic capacity of the GTA nanocomposites.

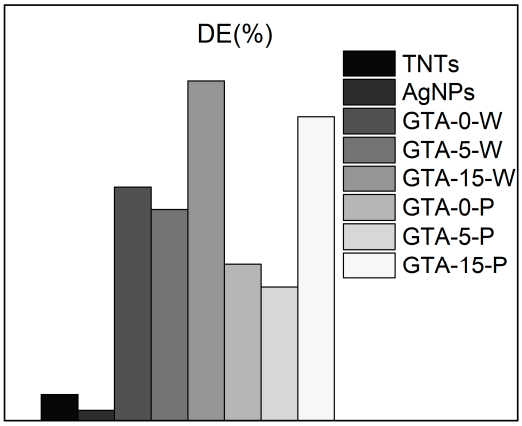

Figure 8. Results of RhB photodecomposition of GTA samples at 0 kGy, 5 kGy, 15 kGy (in water, in PEG) and precursors.

4. Conclusions

In this study, we demonstrated the feasibility of synthesizing the GTA nanocomposite, consisting of GO, TNTs, and AgNPs, using a straightforward aqueous method employing γ-irradiation. This technique relies on the radiolysis of water, which generates highly reactive reducing and oxidizing species upon interaction with γ-rays. By employing PEG, the oxidizing species were scavenged, creating a majorly reducing environment that unfavorably influenced the interactions within the GTA nanocomposite. This synthesis approach facilitated the attachment of TNTs and AgNPs onto the GO scaffold. Additionally, our results revealed that the material exhibited outstanding dye-degrading activity when exposed to natural sunlight as the radiation source, surpassing the performance of individual components. This work highlights the potential of γ-irradiation as a simple method for the production of well-dispersed nanoparticles on the aforementioned support.

Author Contributions: Resources, A.P.T.N.; Writing—original draft, A.P.T.N.; Writing—review & editing, T.T.T.N.; Visualization, A.P.T.N.; Project administration, K.D.N.V.; Funding acquisition, K.D.N.V. All authors have read and agreed to the published version of the manuscript.

Funding: This research was funded by the project of the Institute of Applied Materials Science, Vietnam Academy of Science and Technology, under Grant Number CSCL19.02/22–23.

Data Availability Statement: The authors declare that the raw data supporting the findings of this study are available in the Google Drive repository with the identifier: https://docs.google.com/spreadsheets/d/15rhErmgEy3XbYSfnIor8iPdR-iaSwdcJ/edit?usp=sharing&ouid=116748305038892110526&rtpof=true&sd=true (accessed on 29 July 2023). Source data are provided by corresponding author upon reasonable request.

Acknowledgments: The project of the Institute of Applied Materials Science, Vietnam Academy of Science and Technology, under Grant Number CSCL19.02/22–23 (for graphene oxide synthesis and sample synthesis under γ-irradiation) is gratefully acknowledged. The authors are grateful to N.V.D. Khang for his help in XRD data recording.

Conflicts of Interest: The authors declare that they have no known competing financial interest or personal relationships that could have appeared to influence the work reported in this paper.

References

1. Singh, M.; Vajpayee, M.; Ledwani, L. Eco-friendly surface modification of natural fibres to improve dye uptake using natural dyes and application of natural dyes in fabric finishing: A review. *Mater. Today Proc.* **2021**, *43*, 2868–2871. [CrossRef]
2. Rastogi, S.; Kesavachandran, C.; Mahdi, F.; Pandey, A. Occupational cancers in leather tanning industries: A short review. *Indian J. Occup. Environ. Med.* **2007**, *11*, 3. [CrossRef] [PubMed]
3. Shang, Y.; Zhang, D.; Liu, Y.; Guo, C. Preliminary comparison of different reduction methods of graphene oxide. *Bull. Mater. Sci.* **2015**, *38*, 7–12. [CrossRef]

4. Lei, X.; You, M.; Pan, F.; Liu, M.; Yang, P.; Xia, D.; Li, Q.; Wang, Y.; Fu, J. $CuFe_2O_4$@ GO nanocomposite as an effective and recoverable catalyst of peroxymonosulfate activation for degradation of aqueous dye pollutants. *Chin. Chem. Lett.* **2019**, *30*, 2216–2220. [CrossRef]
5. Zhao, D.; Sheng, G.; Chen, C.; Wang, X. Enhanced photocatalytic degradation of methylene blue under visible irradiation on graphene@ TiO_2 dyade structure. *Appl. Catal. B Environ.* **2012**, *111*, 303–308. [CrossRef]
6. Kumari, S.; Sharma, P.; Yadav, S.; Kumar, J.; Vij, A.; Rawat, P.; Kumar, S.; Sinha, C.; Bhattacharya, J.; Srivastava, C.M. A novel synthesis of the graphene oxide-silver (GO-Ag) nanocomposite for unique physiochemical applications. *ACS Omega* **2020**, *5*, 5041–5047. [CrossRef]
7. Nguyen, S.V.; Duong, T.T.D.; Nguyen, P.T.; Le, N.T.S. Reduction of graphene oxide by TiO_2 nanotubes photocatalyst. *VNUHCM J. Sci. Technol. Dev.* **2015**, *18*, 228–236. [CrossRef]
8. Nischk, M.; Mazierski, P.; Wei, Z.; Siuzdak, K.; Kouame, N.A.; Kowalska, E.; Remita, H.; Zaleska-Medynska, A. Enhanced photocatalytic, electrochemical and photoelectrochemical properties of TiO_2 nanotubes arrays modified with Cu, AgCu and Bi nanoparticles obtained via radiolytic reduction. *Appl. Surf. Sci.* **2016**, *387*, 89–102. [CrossRef]
9. Zhao, F.; Dong, B.; Gao, R.; Su, G.; Liu, W.; Shi, L.; Xia, C.; Cao, L. A three-dimensional graphene-TiO_2 nanotube nanocomposite with exceptional photocatalytic activity for dye degradation. *Appl. Surf. Sci.* **2015**, *351*, 303–308. [CrossRef]
10. Sandoval, A.; Hernandez-Ventura, C.; Klimova, T.E. Titanate nanotubes for removal of methylene blue dye by combined adsorption and photocatalysis. *Fuel* **2017**, *198*, 22–30. [CrossRef]
11. Chen, M.; Sun, T.; Zhao, W.; Yang, X.; Chang, W.; Qian, X.; Yang, Q.; Chen, Z. In Situ Growth of Metallic 1T-MoS_2 on TiO_2 Nanotubes with Improved Photocatalytic Performance. *ACS Omega* **2021**, *6*, 12787–12793. [CrossRef] [PubMed]
12. Martínez-Orozco, R.D.; Rosu, H.; Lee, S.-W.; Rodríguez-González, V. Understanding the adsorptive and photoactivity properties of Ag-graphene oxide nanocomposites. *J. Hazard. Mater.* **2013**, *263*, 52–60. [CrossRef] [PubMed]
13. Wang, N.; Guan, B.; Zhao, Y.; Zou, Y.; Geng, G.; Chen, P.; Wang, F.; Liu, M. Sub-10 nm Ag nanoparticles/graphene oxide: Controllable synthesis, size-dependent and extremely ultrahigh catalytic activity. *Small* **2019**, *15*, 1901701. [CrossRef] [PubMed]
14. Raliya, R.; Avery, C.; Chakrabarti, S.; Biswas, P. Photocatalytic degradation of methyl orange dye by pristine titanium dioxide, zinc oxide, and graphene oxide nanostructures and their composites under visible light irradiation. *Appl. Nanosci.* **2017**, *7*, 253–259. [CrossRef]
15. Gao, W.; Wang, M.; Ran, C.; Yao, X.; Yang, H.; Liu, J.; He, D.; Bai, J. One-pot synthesis of Ag/r-GO/TiO_2 nanocomposites with high solar absorption and enhanced anti-recombination in photocatalytic applications. *Nanoscale* **2014**, *6*, 5498–5508. [CrossRef]
16. Vasilaki, E.; Georgaki, I.; Vernardou, D.; Vamvakaki, M.; Katsarakis, N. Ag-loaded TiO_2/reduced graphene oxide nanocomposites for enhanced visible-light photocatalytic activity. *Appl. Surf. Sci.* **2015**, *353*, 865–872. [CrossRef]
17. Le Caër, S. Water radiolysis: Influence of oxide surfaces on H2 production under ionizing radiation. *Water* **2011**, *3*, 235–253. [CrossRef]
18. Al-Assaf, S.; Coqueret, X.; Zaman, H.M.D.K.; Sen, M.; Ulański, P. *The Radiation Chemistry of Polysaccharides*; International Atomic Energy Agency Vienna: Wien, Austria, 2016.
19. Vo, K.D.N.; Kowandy, C.; Dupont, L.; Coqueret, X.; Hien, N.Q. Radiation synthesis of chitosan stabilized gold nanoparticles comparison between e−beam and γ irradiation. *Radiat. Phys. Chem.* **2014**, *94*, 84–87. [CrossRef]
20. Zhang, B.; Li, L.; Wang, Z.; Xie, S.; Zhang, Y.; Shen, Y.; Yu, M.; Deng, B.; Huang, Q.; Fan, C. Radiation induced reduction: An effective and clean route to synthesize functionalized graphene. *J. Mater. Chem.* **2012**, *22*, 7775–7781. [CrossRef]
21. Divya, K.; Chandran, A.; Reethu, V.; Mathew, S. Enhanced photocatalytic performance of RGO/Ag nanocomposites produced via a facile microwave irradiation for the degradation of Rhodamine B in aqueous solution. *Appl. Surf. Sci.* **2018**, *444*, 811–818. [CrossRef]
22. Wang, T.; Tang, T.; Gao, Y.; Chen, Q.; Zhang, Z.; Bian, H. Hydrothermal preparation of Ag-TiO_2-reduced graphene oxide ternary microspheres structure composite for enhancing photocatalytic activity. *Phys. E Low-Dimens. Syst. Nanostructures* **2019**, *112*, 128–136. [CrossRef]
23. Nguyen, K.D.V.; Vo, K.D.N. Magnetite nanoparticles-TiO_2 nanoparticles-graphene oxide nanocomposite: Synthesis, characterization and photocatalytic degradation for Rhodamine-B dye. *AIMS Mater. Sci.* **2020**, *7*, 288–301. [CrossRef]
24. Zavala, M.Á.L.; Morales, S.A.L.; Ávila-Santos, M. Synthesis of stable TiO_2 nanotubes: Effect of hydrothermal treatment, acid washing and annealing temperature. *Heliyon* **2017**, *3*, e00456. [CrossRef]
25. KELLY, J.M. Triangular silver nanoparticles: Their preparation, functionalisation and properties. *Acta Phys. Pol. A* **2012**, *122*, 337–345. [CrossRef]
26. Marcano, D.C.; Kosynkin, D.V.; Berlin, J.M.; Sinitskii, A.; Sun, Z.; Slesarev, A.; Alemany, L.B.; Lu, W.; Tour, J.M. Improved synthesis of graphene oxide. *ACS Nano* **2010**, *4*, 4806–4814. [CrossRef]
27. Wang, G.; Chang, J.; Tang, W.; Xie, W.; Ang, Y.S. 2D materials and heterostructures for photocatalytic water-splitting: A theoretical perspective. *J. Phys. D Appl. Phys.* **2022**, *55*, 293002. [CrossRef]
28. Lops, C.; Ancona, A.; Di Cesare, K.; Dumontel, B.; Garino, N.; Canavese, G.; Hérnandez, S.; Cauda, V. Sonophotocatalytic degradation mechanisms of Rhodamine B dye via radicals generation by micro-and nano-particles of ZnO. *Appl. Catal. B Environ.* **2019**, *243*, 629–640. [CrossRef] [PubMed]
29. Song, J.; Wang, X.; Chang, C.-T. Preparation and characterization of graphene oxide. *J. Nanomater.* **2014**, *2014*, 276143. [CrossRef]

30. El-Batal, A.; Sidkey, N.M.; Ismail, A.; Arafa, R.A.; Fathy, R.M. Impact of silver and selenium nanoparticles synthesized by gamma irradiation and their physiological response on early blight disease of potato. *J. Chem. Pharm. Res.* **2016**, *8*, 934–951.
31. Meng, R.; Hou, H.; Liu, X.; Duan, J.; Liu, S. Binder-free combination of graphene nanosheets with TiO_2 nanotube arrays for lithium ion battery anode. *J. Porous Mater.* **2016**, *23*, 569–575. [CrossRef]
32. Wang, S.; Zhang, Y.; Ma, H.-L.; Zhang, Q.; Xu, W.; Peng, J.; Li, J.; Yu, Z.-Z.; Zhai, M. Ionic-liquid-assisted facile synthesis of silver nanoparticle-reduced graphene oxide hybrids by gamma irradiation. *Carbon* **2013**, *55*, 245–252. [CrossRef]
33. Manalu, S.P.; Natarajan, T.S.; De Guzman, M.; Wang, Y.-F.; Chang, T.-C.; Yen, F.-C.; You, S.-J. Synthesis of ternary g-C_3N_4/Bi_2MoO_6/TiO_2 nanotube composite photocatalysts for the decolorization of dyes under visible light and direct sunlight irradiation. *Green Process. Synth.* **2018**, *7*, 493–505. [CrossRef]
34. Chaiyakun, S.; Witit-Anun, N.; Nuntawong, N.; Chindaudom, P.; Oaew, S.; Kedkeaw, C.; Limsuwan, P. Preparation and characterization of graphene oxide nanosheets. *Procedia Eng.* **2012**, *32*, 759–764.
35. Gupta, B.; Kumar, N.; Panda, K.; Melvin, A.A.; Joshi, S.; Dash, S.; Tyagi, A.K. Effective noncovalent functionalization of poly (ethylene glycol) to reduced graphene oxide nanosheets through γ-radiolysis for enhanced lubrication. *J. Phys. Chem. C* **2016**, *120*, 2139–2148. [CrossRef]
36. Diak, M.; Klein, M.; Klimczuk, T.; Lisowski, W.; Remita, H.; Zaleska-Medynska, A.; Grabowska, E. Photoactivity of decahedral TiO_2 loaded with bimetallic nanoparticles: Degradation pathway of phenol-1-13C and hydroxyl radical formation. *Appl. Catal. B Environ.* **2017**, *200*, 56–71. [CrossRef]
37. Wu, J.-B.; Lin, M.-L.; Cong, X.; Liu, H.-N.; Tan, P.-H. Raman spectroscopy of graphene-based materials and its applications in related devices. *Chem. Soc. Rev.* **2018**, *47*, 1822–1873. [CrossRef] [PubMed]
38. Phan, T.D.; Vo, C.M.; Tran, T.M.T.; Luu, T.L.A.; Nguyen, X.S. Structural and bandgap properties of titanium dioxide nanotube/graphene oxide composites prepared by a facile hydrothermal method. *Mater. Res. Express* **2019**, *6*, 105054. [CrossRef]
39. Van Viet, P.; Phan, B.T.; Mott, D.; Maenosono, S.; Sang, T.T.; Thi, C.M. Silver nanoparticle loaded TiO_2 nanotubes with high photocatalytic and antibacterial activity synthesized by photoreduction method. *J. Photochem. Photobiol. A Chem.* **2018**, *352*, 106–112. [CrossRef]
40. Bellardita, M.; Di Paola, A.; Megna, B.; Palmisano, L. Absolute crystallinity and photocatalytic activity of brookite TiO_2 samples. *Appl. Catal. B Environ.* **2017**, *201*, 150–158. [CrossRef]
41. Yue, Y.; Zhou, B.; Shi, J.; Chen, C.; Li, N.; Xu, Z.; Liu, L.; Kuang, L.; Ma, M.; Fu, H. γ-Irradiation assisted synthesis of graphene oxide sheets supported Ag nanoparticles with single crystalline structure and parabolic distribution from interlamellar limitation. *Appl. Surf. Sci.* **2017**, *403*, 282–293. [CrossRef]
42. Adly, M.; El-Dafrawy, S.M.; El-Hakam, S. Application of nanostructured graphene oxide/titanium dioxide composites for photocatalytic degradation of rhodamine B and acid green 25 dyes. *J. Mater. Res. Technol.* **2019**, *8*, 5610–5622. [CrossRef]
43. Zhang, Q.; Ye, S.; Chen, X.; Song, X.; Li, L.; Huang, X. Photocatalytic degradation of ethylene using titanium dioxide nanotube arrays with Ag and reduced graphene oxide irradiated by γ-ray radiolysis. *Appl. Catal. B Environ.* **2017**, *203*, 673–683. [CrossRef]